Iranian Journal of Basic Medical Sciences
ijbms.mums.ac.ir

Neuroprotective effects of ROCK inhibition on hippocampal energy metabolism in a rat model of metabolic syndrome

Nikoloz Zhgenti [1, 2]*, Otar Bibilashvili [1], Irina Petriashvili [3], Nana Koshoridze [1]

[1] Department of Biology, Faculty of Exact and Natural Sciences, Iv. Javakhishvili Tbilisi State University, Tbilisi, Georgia
[2] Faculty of Medicine, Iv. Javakhishvili Tbilisi State University, Tbilisi, Georgian
[3] Department of Pharmacology, Faculty of Medicine, Iv. Javakhishvili Tbilisi State University, Tbilisi, Georgia

ARTICLE INFO

Article type:
Original

Article history:
Received: Dec 30, 2025
Accepted: May 11, 2026

Keywords:
Energy metabolism
Fasudil
Hippocampus metabolic syndrome
Neuroprotection
PI3K/AKT/mTOR
Rho-kinase (ROCK)

ABSTRACT

Objective(s): Metabolic syndrome (MS) is associated with insulin resistance, hyperglycemia, and dyslipidemia, leading to impaired neuronal energy metabolism and hippocampal dysfunction. Rho-associated kinase (ROCK) has been implicated in metabolic and neuroinflammatory dysregulation; however, its role in MS-induced hippocampal energy imbalance remains unclear. This study aimed to determine whether pharmacological ROCK inhibition with fasudil restores hippocampal energy metabolism in a rat model of fructose-induced MS.

Materials and Methods: Male Lewis rats were divided into control, MS, and MS+fasudil groups. Plasma and hippocampal metabolic parameters were assessed using biochemical assays. Activities of glycolytic enzymes, Krebs cycle enzymes, and mitochondrial respiratory chain complexes I–IV were measured. Phosphatidylinositol 3-kinase/Protein kinase B/Mechanistic target of rapamycin (PI3K/AKT/mTOR) pathway components, including phosphorylated PI3K, AKT, mTOR, Phosphatase and tensin homolog (PTEN), and Ras homolog enriched in brain (Rheb), were analyzed by Western blotting.

Results: MS disrupted glucose homeostasis and significantly suppressed the activities of glycolytic, mitochondrial, and respiratory chain enzymes in the hippocampus. These changes were accompanied by reduced phosphorylation of PI3K, AKT, and mTOR, increased PTEN expression, and decreased Rheb levels, indicating impaired PI3K/AKT/mTOR signaling. Fasudil treatment normalized plasma and hippocampal glucose levels, restored enzymatic activities across major energy-producing pathways, and reactivated PI3K/AKT/mTOR signaling by reducing PTEN and restoring AKT and Rheb activity.

Conclusion: These findings demonstrate that ROCK overactivation contributes to central insulin resistance and hippocampal energy dysfunction in MS. ROCK inhibition with fasudil effectively reverses these alterations, highlighting ROCK as a potential therapeutic target for preserving hippocampal metabolic function in MS.

▶Please cite this article as:
Zhgenti N, Bibilashvili O, Petriashvili I, Koshoridze N. Neuroprotective effects of ROCK inhibition on hippocampal energy metabolism in a rat model of metabolic syndrome. Iran J Basic Med Sci. 2026; 29:

Introduction

Metabolic syndrome (MS) is a cluster of interrelated metabolic disorders, including obesity, dyslipidemia, hyperglycemia, insulin resistance, and arterial hypertension, which collectively increase the risk of type 2 diabetes mellitus, cardiovascular diseases such as myocardial infarction, cerebrovascular disorders, and non-alcoholic fatty liver disease (1-4). Epidemiological data indicate that, as of 2020, MS affected approximately 3% of children and 5% of adolescents worldwide (5), while in 2012, its prevalence among the global adult population was estimated at around 35% (6). In recent years, increasing attention has been paid to the effects of MS on the central nervous system (CNS) (7, 8). Clinical studies have demonstrated that individuals with MS exhibit structural and functional alterations in the brain, including hippocampal atrophy, cognitive impairment, mood disturbances, and an elevated risk of neurodegenerative disorders such as Alzheimer's disease (9-11). Consistent with these findings, neuroinflammatory and neurodegenerative changes have also been observed in animal models of MS (12, 13). The brain is particularly susceptible to the systemic disturbances associated with MS, given its high dependence on glucose metabolism and vulnerability to oxidative stress and inflammation. Insulin resistance, one of the hallmark features of MS, impairs neuronal glucose uptake, thereby disrupting cellular energy metabolism, and concurrently alters insulin-dependent signaling cascades, leading to deficits in neuroplasticity, neurotransmission, and neurogenesis (14-16). Furthermore, the chronic oxidative stress and neuroinflammatory responses accompanying these changes damage neurons, glial cells, and the integrity of the blood-brain barrier (17, 18). Collectively, these findings underscore the urgent need to develop novel therapeutic strategies that target the molecular mechanisms underlying the neuropathological consequences of MS, rather than focusing solely on symptomatic treatment.

The hippocampus is particularly vulnerable to insulin

***Corresponding author:** Nikoloz Zhgenti. Chair of Biochemistry, Department of Biology, Faculty of Exact and Natural Sciences, Iv. Javakhishvili Tbilisi State University, Tbilisi, Georgia, Faculty of Medicine, Iv. Javakhishvili Tbilisi State University, Tbilisi, Georgia. Email: nikoloz.zhgenti@tsu.ge

resistance due to its high density of insulin receptors and its critical dependence on insulin-sensitive signaling pathways for metabolic regulation and synaptic plasticity (19-21). Beyond its established role in learning and memory, the hippocampus functions as an important metabolic sensor, integrating peripheral metabolic signals with central neuroendocrine responses. Insulin signaling within hippocampal neurons regulates glucose utilization, mitochondrial function, and the activity of key intracellular pathways such as phosphoinositide 3-kinase (PI3K)/protein kinase B (AKT) and mechanistic target of rapamycin (mTOR), which are essential for protein synthesis, dendritic spine remodeling, and long-term potentiation. Disruption of these pathways during insulin resistance impairs synaptic plasticity, reduces neurogenesis in the dentate gyrus, and promotes neuroinflammatory responses, thereby contributing to cognitive decline (22, 23). Moreover, the hippocampus participates in hypothalamic–pituitary–adrenal axis modulation and systemic energy homeostasis, further linking metabolic dysregulation to structural and functional hippocampal alterations (24). These features collectively explain the selective susceptibility of the hippocampus to MS–associated insulin resistance.

One of the key signaling pathways regulating the structural and metabolic functions of the nervous system is the RhoA/Rho-kinase (ROCK) pathway. ROCK exists in two isoforms, ROCK1 and ROCK2, both of which play essential roles in cytoskeletal dynamics, vascular tone regulation, endothelial permeability, and cell survival (25-27). Importantly, ROCK has been strongly implicated in neuroinflammatory and neurodegenerative processes (28-30). Increased ROCK activity promotes the production of proinflammatory mediators and cytokines, microglial activation, disruption of the neurovascular unit, and neuronal apoptosis (31). Fasudil, a selective ROCK inhibitor clinically used in Japan and China for the treatment of cerebral vasospasm, has gained substantial interest as a neuroprotective agent. In addition to improving cerebral blood flow and reducing ROCK-dependent vasoconstriction, fasudil demonstrates the capacity to modulate cytoskeletal stability, endothelial barrier function, and microglial reactivity. Experimental studies in models of stroke, Alzheimer's disease, and Parkinson's disease indicate that fasudil may attenuate neuronal damage and promote functional recovery, suggesting its broad potential in CNS disorders (32-36). Notably, despite these promising observations, the effects of fasudil on metabolic dysfunction–related brain alterations remain poorly understood. Thus, further research is required to elucidate whether pharmacological inhibition of ROCK by fasudil can counteract the neurobiological consequences of MS and restore disrupted metabolic and signaling pathways in the brain.

Materials and Methods

Study design

The research was conducted on 60 male specific pathogen-free Lewis laboratory rats, aged 8 weeks and weighing 250±10 g. The animals were housed, cared for, and tested in accordance with the Guide for the Care and Use of Laboratory Animals, 2021 (37) at the Department of Biology, Iv. Javakhishvili Tbilisi State University and its vivarium. Throughout the study, the rats had unrestricted access to both water and standard laboratory-grade food (LabDiet, Cat# 5001). The ambient room temperature was rigorously maintained at 22±2 °C to ensure a stable and comfortable environment for the animals. Furthermore, the rats were subjected to a controlled 12-hr light-dark cycle to mimic their natural circadian rhythm. Before the commencement of any experimental procedures, the rats were given 7 days to acclimatize to the vivarium conditions. Following this adaptation phase, they were systematically partitioned into three distinct experimental groups, each composed of 20 rats (Figure 1):

- Group I (Control): Animals received a standard laboratory diet and tap water ad libitum for 60 days. Subsequently, they were administered daily intraperitoneal injections of 0.9% sterile NaCl (100 µl) for 14 consecutive days.
- Group II (Metabolic Syndrome Model): Animals were fed a standard laboratory diet, while their drinking water was replaced with a 30% fructose solution for 60 days to induce metabolic syndrome–like conditions. Following this period, they received daily intraperitoneal injections of 0.9% sterile NaCl (100 µl) for 14 days.
- Group III (Fasudil-Treated): Animals were subjected to the same 30% fructose feeding protocol for 60 days and then treated with daily intraperitoneal injections of fasudil (10 mg/kg, dissolved in sterile 0.9% NaCl; 100 µl per injection) for 14 consecutive days.

On the 74th day of the study, the animals from each group were euthanized in accordance with international guidelines

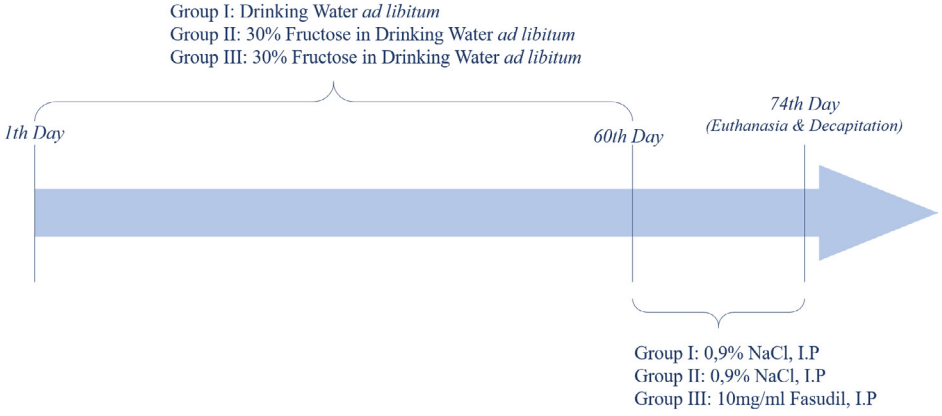

Figure 1. Schematic representation of the study design

(AVMA Guidelines for the Euthanasia of Animals: 2020 Edition) (38). After euthanizing the animals, we decapitated them. Then, their brains were removed and frozen at -80 ˚C. Using the rodent brain coronal matrix (RBMS-200C), stereomicroscope (Laxco LMS-Z230PMZS33), and rat brain atlas (39), we dissected the Hippocampus.

Subcellular fractionation

Subcellular fractionation was performed using a procedure similar to the method described in previous studies (40, 41).

Determination of glucose concentration in hippocampal cells and plasma

To determine glucose concentration in plasma and cytosolic fraction of hippocampus cells, we used a kit provided by Mybiosource (MBS8243232).

Determination of liver dysfunction and dyslipidemia

To assess liver dysfunction and dyslipidemia as a component of MS, plasma lipid profiles and the activities of alanine aminotransferase (ALT) and aspartate aminotransferase (AST) were measured in experimental animals. The following assay kits (MyBioSource) were used: LDL (MBS2540573), HDL (MBS168359), total cholesterol (MBS8305378), triglycerides (MBS9719080), ALT (MBS2540581), and AST (MBS2540582).

Behavioral assessments

To evaluate locomotor activity, exploratory behavior, and hippocampus-dependent spatial working memory, animals were subjected to the Open Field test and the T-maze spontaneous alternation task. Behavioral testing was performed during the light phase of the light/dark cycle under controlled environmental conditions (22±2 ˚C; 50-60% humidity). Animals were habituated to the testing room for at least 30 min prior to the experiments. All apparatuses were cleaned with 70% ethanol between trials to eliminate olfactory cues.

Open field test

The Open Field test was used to assess general locomotor activity and anxiety-like behavior. The apparatus consisted of a square arena (e.g., 50×50×40 cm) with opaque walls and a non-reflective floor divided virtually into peripheral and central zones. Each animal was placed individually in the center of the arena and allowed to explore freely for 5-10 minutes.

The following parameters were analyzed: total distance traveled (cm), time spent in the central zone (s). Total distance traveled was used as an indicator of locomotor activity, whereas time spent in the center was interpreted as an index of anxiety-related behavior. The Open Field test was conducted prior to cognitive testing to exclude confounding effects of altered locomotion.

T-maze spontaneous alternation test

Spatial working memory was assessed using a T-maze spontaneous alternation paradigm, which is sensitive to hippocampal function. The T-maze consisted of three arms of equal dimensions (e.g., 40 cm length×10 cm width×20 cm height), arranged in a T configuration. At the beginning of each trial, the animal was placed in the start arm and allowed to choose freely between the two goal arms.

For spontaneous alternation assessment, each animal underwent a series of consecutive trials (e.g., 5-10 trials), separated by short inter-trial intervals (approximately 30-60 s). An alternation was defined as entry into the arm opposite to the one visited in the previous trial. The percentage of spontaneous alternation was calculated as:

$$\text{Spontaneous alternation (\%)} = \left(\frac{\text{Number of alternations}}{\text{Total possible alternations}}\right) \times 100$$

Total arm entries were also recorded to control for locomotor activity. Increased alternation percentage was interpreted as improved spatial working memory performance.

Determination of energetic metabolism enzyme activity

To assess the functional state of glycolytic metabolism, the activities of key regulatory enzymes were determined. The activity of hexokinase, which catalyzes the phosphorylation of glucose to glucose-6-phosphate and represents the first irreversible step of glycolysis, was measured using a commercial assay kit according to the manufacturer's instructions (MBS719202). The activity of phosphofructokinase, the principal rate-limiting enzyme responsible for the conversion of fructose-6-phosphate to fructose-1,6-bisphosphate, was assessed using a specific assay kit under optimized reaction conditions (MBS8243182). The terminal glycolytic enzyme, pyruvate kinase, catalyzing the conversion of phosphoenolpyruvate to pyruvate with concomitant ATP generation, was analyzed in a similar manner (MBS9719073).

To evaluate the coupling between glycolysis and oxidative metabolism, the activity of pyruvate dehydrogenase, a multienzyme complex that mediates the oxidative decarboxylation of pyruvate to acetyl-CoA, was determined using the Pyruvate Dehydrogenase Activity Assay Kit (MyBioSource, MBS8243249). All measurements were performed according to the respective manufacturer's protocols, and the resulting enzymatic activities were expressed in units per milligram of protein.

To further examine the TCA cycle, we quantified the activities of several critical enzymes, including citrate synthase (MBS9719200), Isocitrate dehydrogenase (MBS8305396), α-ketoglutarate dehydrogenase (MBS8309683), succinate dehydrogenase (MBS8243220), fumarase (MBS7218132), and malate dehydrogenase (MBS8309689), each using their respective assay kits. These measurements provided an integrated view of the glycolytic and TCA cycle enzyme functionality.

To characterize mitochondrial ATP production more comprehensively, we examined the activities of the main complexes of the electron transport chain (ETC). Complex I (NADH: ubiquinone oxidoreductase) activity was determined using the MyBioSource kit (MBS8806971), while Complex II (succinate dehydrogenase) was assayed with kit MBS8243220. The activity of Complex III (cytochrome bc1 complex) was measured using the Complex III Test Kit (MBS3805803). Finally, Complex IV (cytochrome c oxidase) was evaluated with the test kit (MBS037447).

PI3K–AKT–mTOR pathway Western blot analysis

Tissue samples from the hippocampus of experimental animals were subjected to western blot analysis following established procedures (42, 43). The following primary

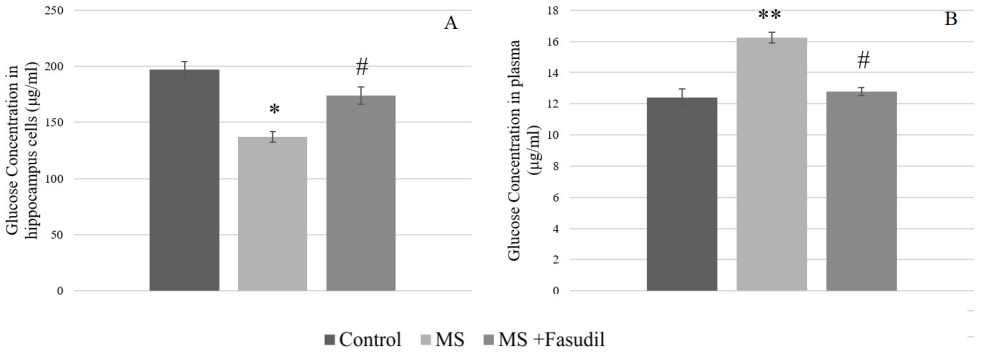

Figure 2. Glucose concentration in hippocampal cells (A) and plasma of rats (B)
Data represent mean±SEM. Statistical analysis was performed using one-way ANOVA followed by Tukey's *post hoc* tests. Significance annotations: $^{*}P\leq0.05$, $^{**}P\leq0.01$, $^{***}P\leq0.001$ compared to the Control group (Group I); $^{\#}P\leq0.05$, $^{\#\#}P\leq0.01$, $^{\#\#\#}P\leq0.001$ compared to the Metabolic Syndrome group (Group II)

antibodies were utilized: PI3K p85 antibody (Cell Signaling, #4292), phospho-PI3K (Tyr458) antibody (Cell Signaling, #4228), AKT antibody (Cell Signaling, #9272), phospho-AKT (Ser473) antibody (Cell Signaling, #9271), mTOR antibody (Cell Signaling, #2983), phospho-mTOR (Ser2448) antibody (Cell Signaling, #2971), PTEN antibody (Cell Signaling, #9559), and Rheb antibody (Cell Signaling, #13879). Immunoreactive proteins were visualized using enhanced chemiluminescence detection (ECL kit, Santa Cruz Biotechnology). Protein concentrations were determined by the bicinchoninic acid (BCA) assay (Thermo Scientific), and band intensities were quantified by densitometric analysis using ImageJ software (NIH, USA). The relative expression levels were normalized to β-actin (Cell Signaling, #4970).

Chemicals and reagents

All the reagents were purchased from Sigma-Aldrich (Sigma-Aldrich Inc., St. Louis, U.S.A.) unless otherwise specified.

Statistical analysis

Data are presented as mean±standard error of the mean (SEM), and statistical analysis was performed using GraphPad Prism 9.0 software (GraphPad Prism 9.0, USA). To assess the assumption of normality, the Shapiro-Wilk test was applied. Only data that met the normality assumption were subjected to further analysis using a one-way ANOVA to determine statistical significance, followed by Tukey's *post hoc* test for multiple comparisons. P-values of 0.05 or less were considered statistically significant.

Results

Glucose concentration changes

As shown in Figure 2 (A, B), plasma glucose concentration was significantly elevated in the metabolic syndrome group compared with controls (F (2, 57)=5.36, $P<0.01$), whereas animals in the third group exhibited a reduction in plasma glucose levels (F (2, 57)=4.10, $P<0.05$). In contrast, glucose concentration in hippocampal cells was significantly decreased in the metabolic syndrome group (F (2, 57)=3.99, $P<0.05$) and increased in the third group (F (2, 57)=4.67, $P<0.05$).

Liver dysfunction and dyslipidemia

Plasma lipid parameters were assessed to evaluate dyslipidemia associated with MS (Figure 3). Group II animals showed significantly increased total cholesterol

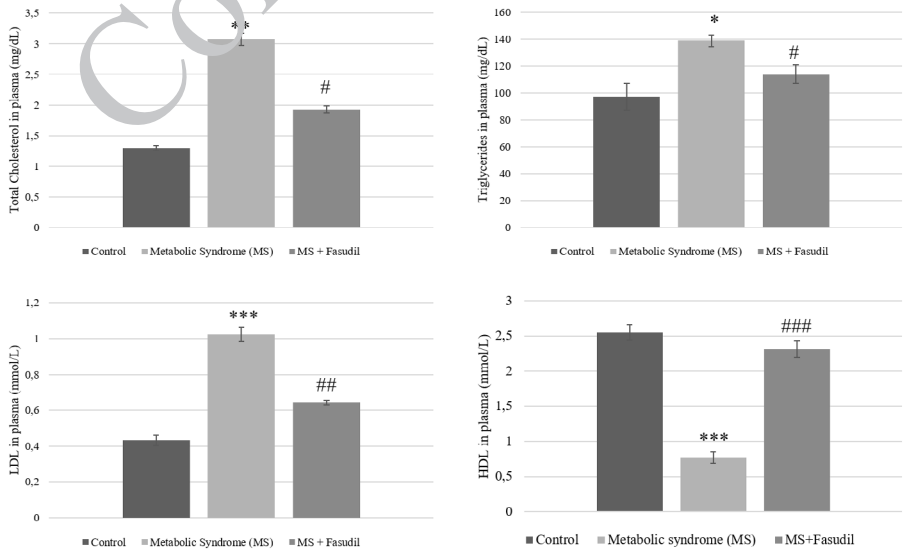

Figure 3. Plasma lipid panel of rats: Concentrations of total cholesterol (A), triglycerides (B), low-density lipoprotein (C), and high-density lipoprotein (D)
Data represent mean±SEM. Statistical analysis was performed using one-way ANOVA followed by Tukey's *post hoc* tests. Significance annotations: $^{*}P\leq0.05$, $^{**}P\leq0.01$, $^{***}P\leq0.001$ compared to the Control group (Group I); $^{\#}P\leq0.05$, $^{\#\#}P\leq0.01$, $^{\#\#\#}P\leq0.001$ compared to the Metabolic Syndrome group (Group II)

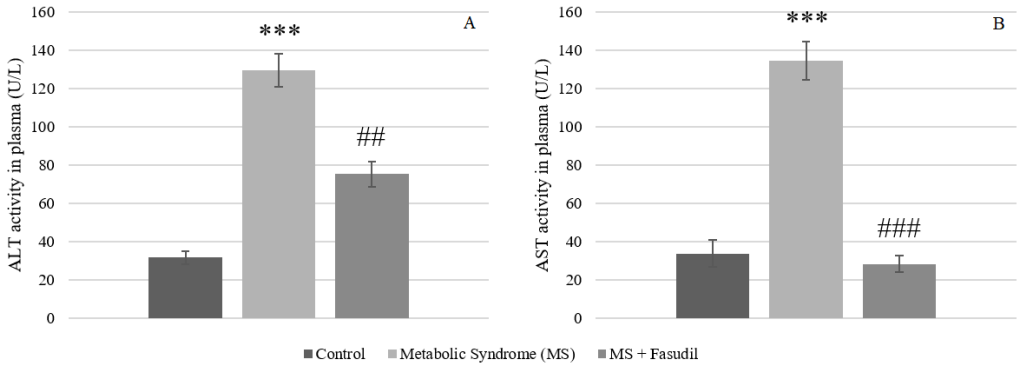

Figure 4. Activity of plasma alanine aminotransferase (A) and aspartate aminotransferase of rats (B)
Data represent mean±SEM. Statistical analysis was performed using one-way ANOVA followed by Tukey's *post hoc* tests. Significance annotations: $^{*}P\leq0.05$, $^{**}P\leq0.01$, $^{***}P\leq0.001$ compared to the Control group (Group I); $^{\#}P\leq0.05$, $^{\#\#}P\leq0.01$, $^{\#\#\#}P\leq0.001$ compared to the Metabolic Syndrome group (Group II)

(F (2, 87)=6.82, P<0.01), triglycerides (F (2, 87)=3.37, P<0.05), and low-density lipoprotein (LDL) levels (F (2, 87)=11.27, P<0.001), together with a significant decrease in high-density lipoprotein (HDL) levels (F (2, 87)=9.48, P<0.001), compared with controls. In Group III, fasudil treatment resulted in significantly lower total cholesterol (F (2, 87)=3.25, P<0.05), triglycerides (F (2, 87)=4.18, P<0.05), and LDL levels (F (2, 87)=5.11, P<0.01), as well as higher HDL concentrations relative to Group II (F (2, 87)=12.44, P<0.001).

Liver function markers were also evaluated (Figure 4). Activities of alanine aminotransferase (ALT)(F (2, 87)=13.04, P<0.001) and aspartate aminotransferase (AST) (F (2, 87)=8.95, P<0.001) were significantly altered among groups. In Group III, fasudil treatment normalized ALT (F (2, 87)=4.99, P<0.01) and AST activities (F (2, 87)=7.34, P<0.001).

Behavioral assessments

Open field

Open Field assessment demonstrated that MS significantly altered locomotor and anxiety-like behavior (Table 1). Total distance traveled was markedly reduced in MS animals compared with controls (F (2, 87)=8.31, P<0.001), indicating decreased exploratory activity. Fasudil treatment partially restored locomotor performance (F (2, 87)=5.22, P<0.01), though values remained slightly below control levels.

Time spent in the center of the arena, an index of anxiety-like behavior, was also significantly decreased in MS animals relative to controls (F (2, 87)=4.97, P<0.01), reflecting increased anxiety. Fasudil treatment improved center exploration (F (2, 87)=7.03, P<0.01), suggesting partial mitigation of anxiety-like behavior. These findings indicate that MS induces both hypoactivity and increased anxiety, which are ameliorated by ROCK inhibition.

T maze

Spatial working memory performance was significantly affected by MS and fasudil treatment (Table 2). Animals in the metabolic syndrome group exhibited a marked reduction in spontaneous alternation compared to controls (F (2, 87) =10.02, P<0.001), indicating impaired hippocampus-dependent working memory. Treatment with fasudil significantly improved cognitive performance compared to untreated MS animals (F (2, 87)=6.51, P<0.01), although values remained slightly lower than control levels. These findings suggest that MS induces significant hippocampal dysfunction, which is partially reversed by ROCK inhibition.

Energy metabolism enzyme activity

The changes in the activities of glycolytic enzymes were not uniform (Figure 5). Hexokinase activity was elevated

Table 2. Change in spontaneous alternations (%) between experimental rats

Group	Mean (%)	SEM	*P*-Value
Group I – Control	74.6	2.4	
Group II – Metabolic Syndrome	49.2	2.1	***
Group III – Metabolic Syndrome+Fasudil	63.8	2.3	##

Data represent mean±SEM. Statistical analysis was performed using one-way ANOVA followed by Tukey's *post hoc* tests. Significance annotations: $^{*}P\leq0.05$, $^{**}P\leq0.01$, $^{***}P\leq0.001$ compared to the Control group (Group I); $^{\#}P\leq0.05$, $^{\#\#}P\leq0.01$, $^{\#\#\#}P\leq0.001$ compared to the Metabolic Syndrome group (Group II)

Table 1. Change in total distance (cm) and time in center (s) between experimental rats

Group	Total Distance (cm)	SEM	*P*-Value	Time in Center (s)	SEM	*P*-Value
Group I – Control	4523	210		38.5	3.2	
Group II – Metabolic Syndrome	3897	185	***	27.2	2.5	**
Group III – Metabolic Syndrome+Fasudil	4221	200	##	34.5	2.8	##

Data represent mean±SEM. Statistical analysis was performed using one-way ANOVA followed by Tukey's *post hoc* tests. Significance annotations: $^{*}P\leq0.05$, $^{**}P\leq0.01$, $^{***}P\leq0.001$ compared to the Control group (Group I); $^{\#}P\leq0.05$, $^{\#\#}P\leq0.01$, $^{\#\#\#}P\leq0.001$ compared to the Metabolic Syndrome group (Group II)

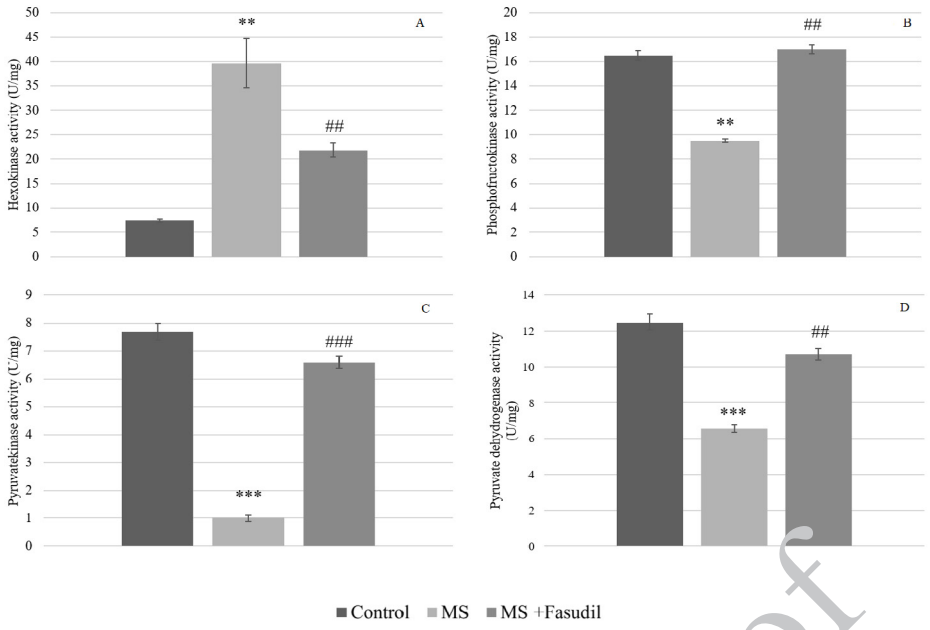

Figure 5. Activity (U/mg) of glycolytic enzymes: Hexokinase (A), Phosphofructokinase (B), Pyruvate kinase (C) and Pyruvate Dehydrogenase in the hippocampal cells of rats (D)
Data represent mean±SEM. Statistical analysis was performed using one-way ANOVA followed by Tukey's *post hoc* tests. Significance annotations: $^{*}P\leq0.05$, $^{**}P\leq0.01$, $^{***}P\leq0.001$ compared to the Control group (Group I); $^{\#}P\leq0.05$, $^{\#\#}P\leq0.01$, $^{\#\#\#}P\leq0.001$ compared to the Metabolic Syndrome group (Group II)

in the metabolic syndrome group (F (2, 57)=6.02, $P<0.01$) and normalized in the fasudil-treated group (F (2, 57)=5.11, $P<0.01$). In contrast, phosphofructokinase (F (2, 57)=5.69, $P<0.01$) and pyruvate kinase (F (2, 57)=9.21, $P<0.001$) activities were decreased in the metabolic syndrome group, while in the fasudil-treated group both enzymes showed significant increases (phosphofructokinase - F (2, 57)=6.74, $P<0.01$, pyruvate kinase - F (2, 57)=8.47, $P<0.001$). Pyruvate dehydrogenase activity was also reduced in the metabolic syndrome group (F (2, 57)=7.56, $P<0.001$) and returned to control levels following fasudil treatment (F (2, 57)=5.50, $P<0.01$).

Regarding the citric acid cycle enzymes (Figure 6), activities of all studied enzymes: citrate synthase (CS)(F

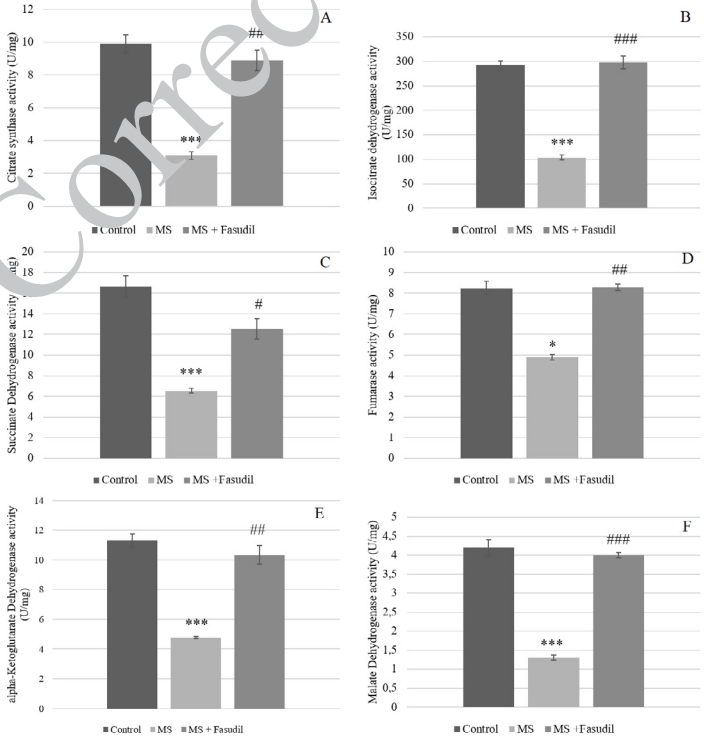

Figure 6. Activity (U/mg) of citrate synthase (A), isocitrate dehydrogenase (B), alpha-ketoglutarate dehydrogenase (C), succinate dehydrogenase (D), Fumarase (E), and Malate Dehydrogenase in the hippocampal cells of rats (F)
Data represent mean±SEM. Statistical analysis was performed using one-way ANOVA followed by Tukey's *post hoc* tests. Significance annotations: $^{*}P\leq0.05$, $^{**}P\leq0.01$, $^{***}P\leq0.001$ compared to the Control group (Group I); $^{\#}P\leq0.05$, $^{\#\#}P\leq0.01$, $^{\#\#\#}P\leq0.001$ compared to the Metabolic Syndrome group (Group II)

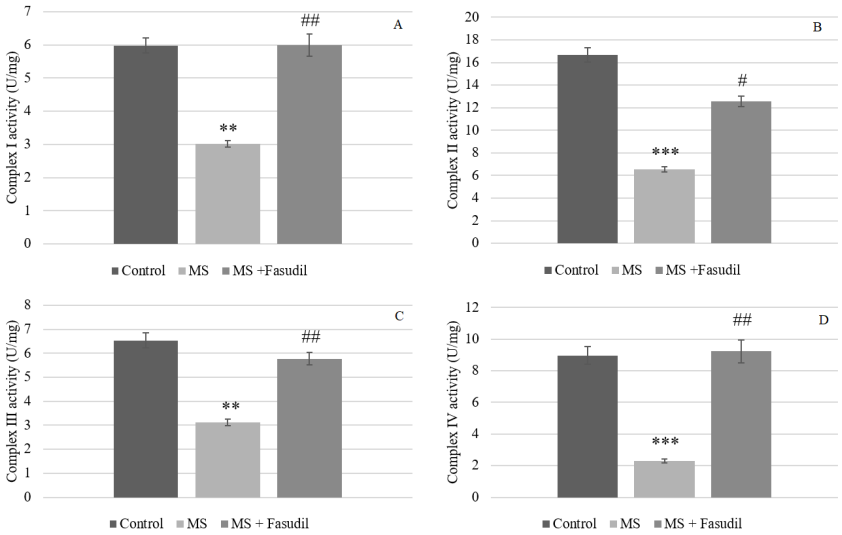

Figure 7. Activity (U/mg) of electron transport chain enzyme complexes: I complex (NADH-dependent dehydrogenase) (A); II complex (succinate dehydrogenase) (B); III complex (cytochrome c reductase) (C); IV complex (cytochrome c oxidase) in the hippocampal cells of rats (D)
Data represent mean±SEM. Statistical analysis was performed using one-way ANOVA followed by Tukey's *post hoc* tests. Significance annotations: $^{*}P\leq0.05$, $^{**}P\leq0.01$, $^{***}P\leq0.001$ compared to the Control group (Group I); $^{\#}P\leq0.05$, $^{\#\#}P\leq0.01$, $^{\#\#\#}P\leq0.001$ compared to the Metabolic Syndrome group (Group II)

(2, 57)=8.66, *P*<0.001), isocitrate dehydrogenase (ICDH) (F (2, 57)=12.15, *P*<0.001), α-ketoglutarate dehydrogenase (αKGDH)(F (2, 57)=10.20, *P*<0.001), succinate dehydrogenase (SDH)(F (2, 57)=8.27, *P*<0.001), fumarase (FH)(F (2, 57)=4.23, *P*<0.05), and malate dehydrogenase (MDH)(F (2, 57)=10.39, *P*<0.001), were significantly decreased in the hippocampus of the metabolic syndrome group. Fasudil treatment (Group III) resulted in partial or complete restoration of the activities of all these enzymes (CS-F (2, 57)=6.33, *P*<0.01; ICDH-F (2, 57)=11.54, *P*<0.001; αKGDH-F (2,57)=7.23, *P*<0.01; SDH-F (2, 57)=4.82, *P*<0.05; FH-F (2, 57)=5.78, *P*<0.01; MDH-F (2, 57)=13.77, *P*<0.001).

Based on the data obtained, it became relevant to study the effects of fasudil on ATP synthesis, in particular by assessing the activity of mitochondrial respiratory chain complexes across all experimental groups. As shown in Figure 7, the activity of all enzyme complexes in the respiratory chain was significantly reduced in metabolic syndrome group animals (Complex I-F(2, 57)=6.80, *P*<0.01; Complex II-F(2,57)=9.16, *P*<0.001; Complex III-F(2,57)=7.08, *P*<0.01; and Complex IV-F(2,57)=11.06, *P*<0.001). After fasudil administration, the function of the electron transport chain approached normal levels (Complex I-F(2,57)=5.87, *P*<0.01; Complex II-F (2, 57)=3.99, *P*<0.05; Complex III-F (2, 57)=7.22, *P*<0.01; and Complex IV-F (2, 57)=6.28, *P*<0.01).

PI3K-AKT-mTOR pathway

It is well established that both intrinsic and extrinsic factors regulate cellular energy metabolism, with the PI3K-AKT-mTOR signaling pathway playing a central role. Based on this, we examined quantitative changes in key components of this pathway in hippocampal cells across the experimental groups. The results are shown in Figure 8. As illustrated, the total (non-phosphorylated) forms of PI3K, AKT, and mTOR remained unchanged. However, the

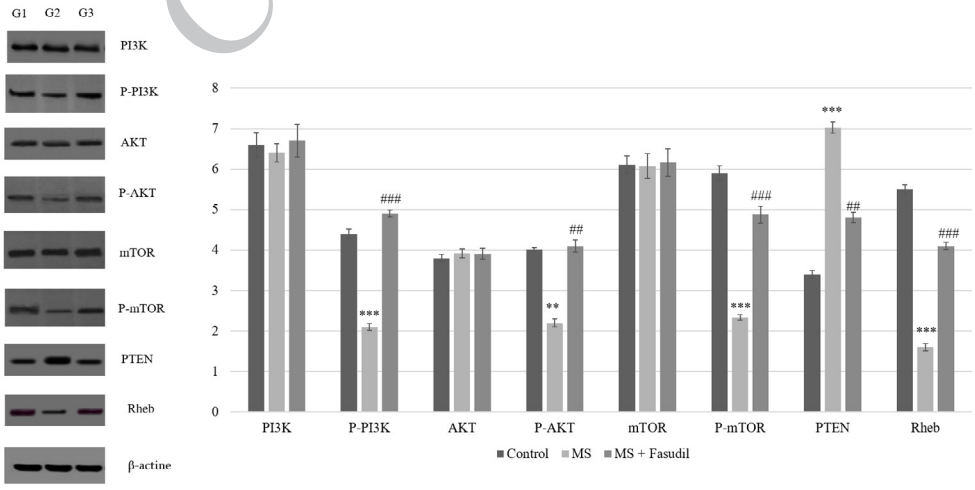

Figure 8. Mean values and representative Western blots of PI3K, p-PI3K (Tyr458), AKT, p-AKT(Serine 473), mTOR, and p-mTOR (Serine 2448), Rheb, and PTEN in the hippocampus cells in the hippocampal cells of rats
Data represent mean±SEM. Statistical analysis was performed using one-way ANOVA followed by Tukey's *post hoc* tests. Significance annotations: $^{*}P\leq0.05$, $^{**}P\leq0.01$, $^{***}P\leq0.001$ compared to the Control group (Group I); $^{\#}P\leq0.05$, $^{\#\#}P\leq0.01$, $^{\#\#\#}P\leq0.001$ compared to the Metabolic Syndrome group (Group II)

phosphorylated forms were significantly altered: p-PI3K ($F(2, 57)=9.15$, $P<0.001$), p-AKT ($F(2, 57)=6.74$, $P<0.01$), and p-mTOR ($F(2, 57)=10.92$, $P<0.001$) were markedly reduced in the metabolic syndrome group (Group II). In contrast, rats in the fasudil-treated group (Group III) exhibited significant increases in the expression of all three phosphorylated proteins (p-PI3K: $F(2, 57)=16.11$, $P<0.001$; p-AKT: $F(2, 57)=7.25$, $P<0.01$; p-mTOR: $F(2, 57)=12.18$, $P<0.001$).

Expression of the PI3K inhibitor PTEN was elevated in the metabolic syndrome group ($F(2, 57)=11.82$, $P<0.001$) and returned to near-control levels following fasudil treatment ($F(2, 57)=7.56$, $P<0.01$). Similarly, the mTOR activator Rheb was decreased in the metabolic syndrome group ($F(2,57)=8.97$, $P<0.001$) and significantly increased in the fasudil-treated group ($F(2, 57)=10.39$, $P<0.001$).

Discussion

This study investigated the neuroprotective role of fasudil, a Rho-kinase (ROCK) inhibitor, against MS-induced energy imbalance in hippocampal cells. Fructose-induced MS disrupted energy homeostasis in hippocampal cells, whereas ROCK inhibition effectively restored it. The pathophysiology of fructose-induced MS in rats is well known and closely linked to the unique hepatic metabolism of fructose, which bypasses the regulatory control of phosphofructokinase and rapidly enters glycolysis downstream, leading to accelerated production of acetyl-CoA and enhanced triglyceride synthesis. Excessive hepatic lipogenesis promotes steatosis and increases LDL secretion into the circulation, resulting in a dyslipidemic profile characterized by elevated triglycerides and reduced HDL levels. Lipid overload in hepatocytes disrupts insulin signaling, contributing to both hepatic and peripheral insulin resistance (44-47). Unlike glucose, fructose does not efficiently stimulate insulin or leptin secretion and fails to suppress ghrelin, resulting in increased caloric intake and positive energy balance (48). Additionally, mitochondrial overload during fructose metabolism elevates reactive oxygen species (ROS) production, triggering oxidative stress and NF-κB–mediated inflammatory responses that further impair metabolic regulation. Consequently, chronic fructose administration in rats induces a phenotype consistent with MS, including hepatic steatosis, hypertriglyceridemia, hyperinsulinemia, insulin resistance, and increased adiposity (49-51).

In the present study, we found that fasudil treatment restored glucose concentrations disrupted by MS in both plasma and hippocampal cells (Figure 2), normalized lipid panel, liver functional tests (ALT, AST) in plasma (Figures 3,4), and increased the activities of glycolytic, Krebs cycle, and respiratory chain enzymes, which were suppressed under MS conditions (Figures 5, 6, 7). An exception is hexokinase, whose activity was increased in rats with MS and normalized upon fasudil treatment, likely reflecting a compensatory response to energy deficiency. In addition, behavioral assessments in the Open Field and T-maze paradigms provided functional evidence of MS-induced hippocampal impairment and its partial rescue by fasudil (Tables 1, 2). MS animals exhibited reduced locomotor activity, increased anxiety-like behavior, and impaired spatial working memory, reflecting hippocampus-dependent deficits likely associated with insulin resistance and disrupted PI3K/AKT/mTOR signaling. Fasudil treatment partially restored locomotor exploration, normalized anxiety indices, and improved spontaneous alternation performance, suggesting that ROCK inhibition can ameliorate both cognitive and emotional deficits.

Our results demonstrate that, in MS, elevated ROCK activity is closely associated with impaired energy metabolism and disrupted insulin signaling in multiple tissues, including the brain (52). Consistent with this, rats with MS in our study exhibited suppression of the PI3K/AKT/mTOR signaling axis, a pathway essential for neuronal survival, synaptic plasticity, and regulation of energy metabolism. This was accompanied by reduced AKT activation, resulting in decreased phosphorylation of downstream targets, diminished mTOR activity, and impaired anabolic processes, which collectively contribute to hippocampal dysfunction. We also observed increased PTEN expression, which further inhibits PI3K/AKT signaling by dephosphorylating PIP_3, and a reduction in Rheb, a direct mTOR activator, further suppressing mTOR signaling and energy homeostasis (Figure 8). Importantly, fasudil-mediated ROCK inhibition in our study normalized these molecular alterations. Treatment reduced PTEN levels toward control values and restored AKT and Rheb activity, thereby reactivating mTOR signaling and reestablishing normal energy metabolism in hippocampal neurons.

ROCK inhibition has been increasingly recognized as a modulatory upstream mechanism influencing the PI3K/AKT/mTOR signaling cascade. Mechanistically, ROCK negatively regulates insulin receptor substrate (IRS) phosphorylation and downstream PI3K activation, thereby limiting AKT phosphorylation and mTOR complex 1 (mTORC1) activity (53, 54). In MS and insulin-resistant states, hyperactivation of ROCK contributes to cytoskeletal stress, endothelial dysfunction, and impaired neuronal insulin signaling, collectively suppressing PI3K/AKT/mTOR pathway activity (55). Moreover, ROCK inhibition can reduce PTEN activity, a key phosphatase that antagonizes PI3K signaling, further facilitating pathway activation (56, 57). These convergent mechanisms provide a plausible explanation for the observed upregulation of PI3K/AKT/mTOR signaling following fasudil treatment, linking ROCK inhibition directly to the restoration of hippocampal metabolic signaling and functional neuroplasticity in MS.

Taken together, our findings indicate that ROCK overactivation directly contributes to central insulin resistance and impaired neuronal energy metabolism in MS, and that pharmacological ROCK inhibition with fasudil can reverse these pathological changes by restoring PI3K/AKT/mTOR pathway integrity.

Despite the promising findings, several limitations should be acknowledged. First, behavioral assessments were limited to the Open Field and T-maze tasks; additional tests, such as novel object recognition or Morris water maze, could provide a more comprehensive evaluation of cognitive and emotional domains. Second, while fasudil-mediated activation of the PI3K/AKT/mTOR pathway was demonstrated, the study did not directly manipulate this pathway to confirm causality between pathway activation and behavioral improvements. Finally, experiments were performed in a single animal model of MS, and extrapolation to other models or to humans requires caution. Addressing these limitations in future studies will strengthen the

mechanistic and translational relevance of ROCK inhibition in MS–associated hippocampal dysfunction.

Conclusion

In conclusion, the present study demonstrates that fructose-induced MS disrupts systemic and hippocampal energy homeostasis, leading to impaired glucose and lipid metabolism, altered liver function, and suppression of key metabolic and survival signaling pathways in the hippocampus. Pharmacological inhibition of ROCK with fasudil effectively reversed these alterations, restoring plasma metabolic parameters, energy metabolism enzyme activities, and PI3K/AKT/mTOR signaling in hippocampal cells. These findings identify ROCK overactivation as a critical mediator of central insulin resistance and neuronal energy imbalance in MS, and highlight fasudil as a potential therapeutic strategy to mitigate MS–associated hippocampal dysfunction.

Our findings demonstrate that fasudil-mediated ROCK inhibition restores hippocampal energy metabolism via PI3K/AKT/mTOR pathway reactivation, providing mechanistic insight into Rho-kinase's role in neuronal dysfunction in metabolic syndrome and highlighting ROCK inhibition as a promising strategy to reverse central metabolic impairment and support neuronal resilience.

Acknowledgment

None.

Ethical Approval

The protocol employed in the study was approved by the Institutional Animal Care and Ethical Committee of Tbilisi State University (NO. 090825).

Funding

This research did not receive any specific grant from funding agencies in the public, commercial, or non-profit sectors.

Authors' Contributions

N Zh conceptualization, project administration, methodology, formal analysis, data curation, visualization, writing– original draft, writing–review & editing, supervision. O B methodology, formal analysis, visualization, supervision. I P conceptualization, project administration, writing–review & editing, data curation, supervision. N K formal analysis, visualization,writing–original draft, writing–review & editing, data curation supervision.

Conflicts of Interest

The authors declare that they have no known competing financial interests or personal relationships that could have appeared to influence the work reported in this paper.

Declaration

During the preparation of this work, the authors used ChatGPT in order to improve language and grammar. After using this tool/service, the authors reviewed and edited the content as needed and take full responsibility for the content of the publication.

References

1. Neeland IJ, Lim S, Tchernof A, Gastaldelli A, Rangaswami J, Ndumele CE, *et al.* Metabolic syndrome. Nat Rev Dis Primers 2024; 10: 77.
2. Eckel RH, Grundy SM, Zimmet PZ. The metabolic syndrome. Lancet 2005; 365: 1415–1428.
3. Rochlani Y, Pothineni NV, Kovelamudi S, Mehta JL. Metabolic syndrome: Pathophysiology, management, and modulation by natural compounds. Ther Adv Cardiovasc Dis 2017; 11: 215-225.
4. Fahed G, Aoun L, Bou Zerdan M, Allam S, Bou Zerdan M, Bouferraa Y, *et al.* Metabolic syndrome: Updates on pathophysiology and management in 2021. Int J Mol Sci 2022; 23: 786.
5. Swarup S, Ahmed I, Grigorova Y, Zeltser R. Metabolic syndrome. In: StatPearls. Treasure Island (FL): StatPearls Publishing; 2025.
6. Noubiap JJ, Nansseu JR, Lontchi-Yimagou E, Nkeck JR, Nyaga UF, Ngouo AT, *et al.* Global, regional, and country estimates of metabolic syndrome burden in children and adolescents in 2020: A systematic review and modelling analysis. Lancet Child Adolesc Health 2022; 6: 158-170.
7. Zouridis S, Nasir AB, Aspichueta P, Syn WK. The link between metabolic syndrome and the brain. Digestion 2025; 106: 203-211.
8. Tahmi M, Palta P, Luchsinger JA. Metabolic syndrome and cognitive function. Curr Cardiol Rep 2021; 23: 180.
9. Zuin M, Roncon L, Passaro A, Cervellati C, Zuliani G. Metabolic syndrome and the risk of late onset Alzheimer's disease: an updated review and meta-analysis. Nutr Metab Cardiovasc Dis 2021; 31: 2244–2252.
10. Al-Kuraishy HM, Jabir MS, Albuhadily AK, Al-Gareeb AI, Rafeeq MF. The link between metabolic syndrome and Alzheimer disease: a mutual relationship and long rigorous investigation. Ageing Res Rev 2023; 91: 102084.
11. Arnoso-Azkurdia M, Ramírez MJ, Solas M. Metabolic syndrome as a risk factor for Alzheimer's disease: A focus on insulin resistance. Int J Mol Sci 2023; 24: 4354.
12. Gómez-Apo E, Mondragón-Maya A, Ferrari-Díaz M, Silva-Pereyra J. Structural brain changes associated with overweight and obesity. J Obes 2021; 2021: 6613385.
13. Fuentes E, Venegas B, Muñoz-Arenas G, Moran C, Vazquez-Roque RA, *et al.* High-carbohydrate and fat diet consumption causes metabolic deterioration, neuronal damage, and loss of recognition memory in rats. J Chem Neuroanat 2023; 129: 102237.
14. de la Monte SM. Insulin resistance and neurodegeneration: Progress towards the development of new therapeutics for Alzheimer's disease. Drugs 2017; 77: 47-65.
15. Kouvari M, D'Cunha NM, Travica N, Sergi D, Zec M, Marx W, *et al.* Metabolic syndrome, cognitive impairment and the role of diet: A narrative review. Nutrients 2022; 14: 333.
16. Chen W, Cai W, Hoover B, Kahn CR. Insulin action in the brain: Cell types, circuits, and diseases. Trends Neurosci 2022; 45: 384–400.
17. Tan BL, Norhaizan ME. Effect of high-fat diets on oxidative stress, cellular inflammatory response and cognitive function. Nutrients 2019; 11: 2579.
18. Candelario-Jalil E, Dijkhuizen RM, Magnus T. Neuroinflammation, stroke, blood-brain barrier dysfunction, and imaging modalities. Stroke 2022; 53: 1473–1486.
19. Grillo CA, Woodruff JL, Macht VA, Reagan LP. Insulin resistance and hippocampal dysfunction: Disentangling peripheral and brain causes from consequences. Exp Neurol 2019; 318: 71-77.
20. Spinelli M, Fusco S, Grassi C. Brain insulin resistance impairs hippocampal plasticity. Vitam Horm 2020; 114: 281-306.
21. Erichsen JM, Woodruff JL, Grillo CA, Piroli GG, Fadel JR, Reagan LP. Hippocampal-specific insulin resistance elicits synaptic effects on glutamate neurotransmission. J Neurochem 2025; 169: e70083.
22. Spinelli M, Fusco S, Grassi C. Brain insulin resistance and hippocampal plasticity: Mechanisms and biomarkers of cognitive decline. Fron Neurosci 2019; 13: 788.
23. He Y, Sun M, Qu M, Lu Y, Yang H, Wang R, *et al.* Brain insulin signaling pathway regulation of hippocampal neuroplasticity in neurocognitive disorders: Mechanisms and therapeutic

implications. J Integr Neurosci 2025; 24: 39446.
24. Battú CE, Rieger D, Loureiro S, Furtado GV, Bock H, Saraiva-Pereira ML, *et al.* Alterations of PI3K and Akt signaling pathways in the hippocampus and hypothalamus of Wistar rats treated with highly palatable food. Nutr Neurosci 2012; 15: 10-17.
25. Yamamoto T, Ugawa Y, Kawamura M, Yamashiro K, Kochi S, Ideguchi H, *et al.* Modulation of microenvironment for controlling the fate of periodontal ligament cells: The role of Rho/ROCK signaling and cytoskeletal dynamics. J Cell Commun Signal 2018; 12: 369-378.
26. Dai C, Khalil RA. Calcium signaling dynamics in vascular cells and their dysregulation in vascular disease. Biomolecules 2025; 15: 892.
27. Koch JC, Tatenhorst L, Roser AE, Saal KA, Tönges L, Lingor P. ROCK inhibition in models of neurodegeneration and its potential for clinical translation. Pharmacol Ther 2018; 189: 1-21.
28. Chong CM, Ai N, Lee SM. ROCK in CNS: Different roles of isoforms and therapeutic target for neurodegenerative disorders. Curr Drug Targets 2017; 18: 455-462.
29. Iyer M, Subramaniam MD, Venkatesan D, Cho SG, Ryding M, Meyer M, *et al.* Role of RhoA-ROCK signaling in Parkinson's disease. Eur J Pharmacol 2021; 894: 173815.
30. Schmidt SI, Blaabjerg M, Freude K, Meyer M. RhoA signaling in neurodegenerative diseases. Cells 2022; 11: 1520.
31. Lu W, Chen Z, Wen J. The role of RhoA/ROCK pathway in the ischemic stroke-induced neuroinflammation. Biomed Pharmacother 2023; 165: 115141.
32. Zhu YT, Zhang Q, Xie HY, Yu KW, Xu GJ, Li SY, *et al.* Environmental enrichment combined with fasudil promotes motor function recovery and axonal regeneration after stroke. Neural Regen Res 2021; 16: 2512-2520.
33. Muraoka S, Izumi T, Nishida K, Chrétien B, Ishii K, Takeuchi I, *et al.* RECOVER study: A multicenter retrospective cohort study and comparison of the efficacy and safety of clazosentan and fasudil in patients with aneurysmal subarachnoid hemorrhage. J Neurosurg 2025; 143: 624–633.
34. Tatenhorst L, Eckermann K, Dambeck V, Fonseca-Ornelas L, Walle H, Lopes da Fonseca T, *et al.* Fasudil attenuates aggregation of α-synuclein in models of Parkinson's disease. Acta Neuropathol Commun 2016; 4: 39.
35. Shibuya M, Hirai S, Seto M, Satoh S, Ohtomo E. Effects of fasudil in acute ischemic stroke: results of a prospective placebo-controlled double-blind trial. J Neurol Sci 2005; 238: 31-39.
36. Dong J, Wang Z, Li L, Zhang M, Wang S, Xiao Y, *et al.* Fasudil alleviates postoperative neurocognitive disorders in mice by downregulating the surface expression of α5GABAAR in hippocampus. CNS Neurosci Ther 2024; 30: e70098.
37. National Research Council (US) Committee for the Update of the Guide for the Care. Guide for the care and use of laboratory animals. 8th ed. Washington, DC: National Academies Press; 2011.
38. American Veterinary Medical Association. AVMA guidelines for the euthanasia of animals. 2020 ed. Schaumburg; 2020.
39. Paxinos G, Watson C. The Rat Brain in Stereotaxic Coordinates. 7th ed. Academic Press; 2014.
40. Zhgenti N, Bibilashvili O, Shengelia M, Burjanadze G, Koshoridze M, Davitashvili E, *et al.* Effect of nicotine on the energy metabolism of substantia nigra cells in MPTP-induced Parkinson's disease. Iran J Basic Med Sci 2025; 28: 1417-1427.
41. Zhgenti N, Bibilashvili O, Burjanadze G, Shengelia M, Koshoridze M, Davitashvili E, *et al.* Dietary plant-derived lectins induce oxidative stress, metabolic dysfunction, apoptosis and neuroinflammation in mice brain. Nutr Neurosci 2025; 28: 1386–1398.
42. Shanshiashvili L, Tsitsilashvili E, Dabrundashvili N, Kalandadze I, Mikeladze D. Metabotropic glutamate receptor 5 may be involved in macrophage plasticity. Biol Res 2017; 50: 4-13.
43. Zhgenti N, Bakuradze E, Bibilashvili O, Koshoridze N. The role of BDNF/PI3K/AKT/Nrf2 signaling in nicotine's protective effects against MPTP-induced Parkinson's disease. Neurosci Lett 2025; 868: 138412.
44. Lubawy M, Formanowicz D. High-fructose diet-induced hyperuricemia accompanying metabolic syndrome-mechanisms and dietary therapy proposals. Int J Environ Res Public Health 2023; 20: 3596.
45. Pan Y, Kong LD. High fructose diet-induced metabolic syndrome: Pathophysiological mechanism and treatment by traditional Chinese medicine. Pharmacol Res 2018; 130: 438-450.
46. Hannou SA, Haslam DE, McKeown NM, Herman MA. Fructose metabolism and metabolic disease. J Clin Invest 2018; 128: 545–555.
47. Softic S, Cohen DE, Kahn CR. Role of dietary fructose and hepatic de novo lipogenesis in fatty liver disease. Dig Dis Sci 2016; 61: 1282–1293.
48. Jung S, Bae H, Song W, Jang C. Dietary fructose and fructose-induced pathologies. Annu Rev Nutr 2022; 42: 45-66.
49. García-Berumen CI, Ortiz-Avila O, Vargas-Vargas MA, Del Rosario-Tamayo BA, Saavedra C, López C, Saavedra-Molina A, *et al.* The severity of rat liver injury by fructose and high fat depends on the degree of respiratory dysfunction and oxidative stress induced in mitochondria. Lipids Health Dis 2019; 18: 78.
50. Cioffi F, Senese R, Lasala P, Ziello A, Mazzoli A, Crescenzo R, *et al.* Fructose-rich diet affects mitochondrial DNA damage and repair in rats. Nutrients 2017; 9: 323.
51. Zhang X, Zhang JH, Chen XY, Hu QH, Wang MX, Jin R, *et al.* Reactive oxygen species-induced TXNIP drives fructose-mediated hepatic inflammation and lipid accumulation through NLRP3 inflammasome activation. Antioxid Redox Signal 2015; 22: 848-870.
52. Huang H, Lee DH, Zabolotny JM, Kim YB. Metabolic actions of Rho-kinase in periphery and brain. Trends Endocrinol Metab 2013; 24: 506-514.
53. Sawada N, Liao JK. Rho/Rho-associated coiled-coil forming kinase pathway as therapeutic targets for statins in atherosclerosis. Antioxid Redox Signal 2014; 20: 1251-1267.
54. Huang H, Lee DH, Zabolotny JM, Kim YB. Metabolic actions of Rho-kinase in periphery and brain. Trends Endocrinol Metab 2013; 24: 506-514.
55. Wei L, Shi J. Insight into rho kinase isoforms in obesity and energy homeostasis. Front Endocrinol 2022; 13: 886534.
56. Li G, Liu L, Shan C, Cheng Q, Budhraja A, Zhou T, *et al.* RhoA/ROCK/PTEN signaling is involved in AT-101-mediated apoptosis in human leukemia cells *in vitro* and *in vivo*. Cell Death Dis 2014; 5: e998.
57. Walker CL, Liu NK, Xu XM. PTEN/PI3K and MAPK signaling in protection and pathology following CNS injuries. Front Biol 2013; 8: 10.